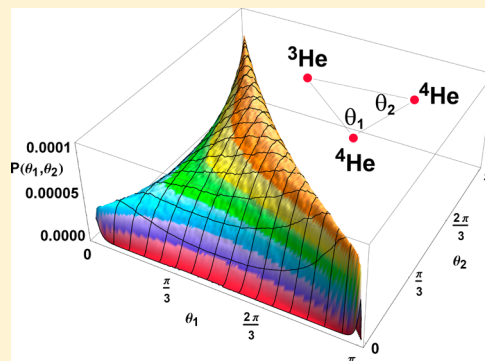


# The Structure of the Asymmetric Helium Trimer $^3\text{He}^4\text{He}_2$

Dario Bressanini\*

Dipartimento di Scienza e Alta Tecnologia, Università dell'Insubria, Via Lucini 3, 22100 Como Italy

**ABSTRACT:** Despite their apparent simplicity, the properties of the two helium trimers,  $^4\text{He}_3$  and  $^3\text{He}^4\text{He}_2$ , are still not completely understood. In particular, the existence of a bound state of the asymmetric trimer  $^3\text{He}^4\text{He}_2$  was established many years ago, using different theoretical approaches, and later it was experimentally detected. However its structural properties have not been thoroughly investigated so far, probably because an accurate theoretical description of this very weakly bound system is computationally quite demanding. In this work we give for the first time an accurate and complete theoretical description of the geometrical structure of this fragile system using quantum Monte Carlo techniques employing the TTY potential and compare its properties with those of  $^4\text{He}_2$  and  $^4\text{He}_3$ . We compute average values of distances and angles, along with the angle–angle distribution function: a two-dimensional probability distribution well suited to discuss the shape of a trimer. Our analysis shows that the lighter isotope is very diffuse and can be found at large distances from the other two atoms, but also close to the center of mass of the system in nearly linear configurations. For this system the concept of “equilibrium structure” is meaningless and all kinds of three-atom configurations must be taken into account in its description.



## INTRODUCTION

In the last few decades weakly bound helium clusters have attracted much attention from both theoreticians and experimentalists.<sup>1</sup> The peculiarities of these systems, caused by the small atomic mass and the very weak interaction potential, coupled with the quantum statistics when more than two  $^3\text{He}$  atoms are present, make them difficult to study theoretically. The existence of the  $^4\text{He}$  dimer was predicted since the 1970s from theoretical studies by many independent calculations (Kolganova et al.<sup>2</sup> provides a recent review of the subject). However, it was only in 1993 that the elusive  $^4\text{He}$  dimer was finally detected by Luo and co-workers<sup>3</sup> in an electron impact ionization experiment. With the availability of modern diffraction techniques from a diffraction grating and the detection of  $^4\text{He}_2$  and  $^4\text{He}_3$  by Schöllkopf and Toennies,<sup>4,5</sup> the study of mixed  $^3\text{He}/^4\text{He}$  clusters and droplets has received a major impetus, both theoretical and experimental.

The accurate description of  $^4\text{He}_3$ , more tightly bound than  $^4\text{He}_2$  but still very diffuse, is not an easy task and is computationally quite demanding. Despite the fact that it has been the subject of many theoretical studies since the early seventies<sup>6</sup> its properties are still not completely understood. For example, still a matter of debate is the possibility that its only excited state is an Efimov state.<sup>2</sup> So far however the experimental evidence of the existence of this state is still missing.<sup>7</sup>

The existence of a bound state of the asymmetric trimer  $^3\text{He}^4\text{He}_2$  was established<sup>8–13</sup> using different theoretical approaches (see the next section for a review of the literature), before it was finally experimentally detected.<sup>14</sup> This trimer however has so far received less theoretical attention than its symmetric counterpart  $^4\text{He}_3$ , and the few scattered papers

published in the literature<sup>8–13,15–21</sup> almost always study the energetics or the scattering observables. The ground state of  $^3\text{He}^4\text{He}_2$  is the only bound state, with an energy 1 order of magnitude smaller than the already weakly bound symmetric trimer  $^4\text{He}_3$ . The difficulty of its theoretical description is probably one of the reasons why a complete investigation of its geometric structure has not been published so far.

In this work we give for the first time an accurate and complete theoretical description of the geometrical structure of this fragile system using quantum Monte Carlo techniques and compare its properties with those of  $^4\text{He}_2$  and  $^4\text{He}_3$ . Performing experiments with  $^3\text{He}$  is quite expensive, due to the higher cost of the lighter helium isotope with respect to the more abundant  $^4\text{He}$ , and an accurate description of its geometrical properties could help experimentalists to devise and interpret new experiments.

## LITERATURE DISCUSSION

In this section we briefly review the few published papers dealing with the asymmetric helium trimer. The energies reported in the reviewed studies are collected in Table 1.

To our knowledge the first studies suggesting that the  $^3\text{He}^4\text{He}_2$  trimer could be bound, albeit employing very primitive pair potentials in their Faddeev type calculations, were done by Duffy and Lim<sup>8</sup> and by Nakaichi et al.<sup>9</sup> Those

**Special Issue:** Franco Gianturco Festschrift

**Received:** March 28, 2014

**Revised:** May 13, 2014

Table 1. Energies of  $^3\text{He}^4\text{He}_2$  Computed with Various Methods and Potentials<sup>a</sup>

energy (cm <sup>-1</sup> )	potential	references	energy (cm <sup>-1</sup> )	potential	references
-0.00710	LM2M2 add-on	Esry et al. <sup>10</sup>	-0.01205	SAPT <sup>c</sup>	Suno et al. <sup>19</sup>
-0.00949	LM2M2	Nielsen et al. <sup>11</sup>	-0.012097	SAPT	Suno et al. <sup>19</sup>
-0.00666(2)	TTY (VMC)	Bressanini et al. <sup>12</sup>	-0.009886	SAPT <sup>b</sup>	Suno et al. <sup>21</sup>
-0.00984(5)	TTY (DMC)	Bressanini et al. <sup>12</sup>	-0.01062	SAPT	Suno et al. <sup>21</sup>
-0.00549(3)	HFD-B(He) (VMC)	Guardiola and Navarro <sup>15</sup>	-0.009964	TTY	Roudnev and Cavagnero <sup>20</sup>
-0.0107(11)	HFD-B(He) (DMC)	Guardiola and Navarro <sup>16</sup>	-0.009983	LM2M2	Roudnev and Cavagnero <sup>20</sup>
-0.00785(3)	TTY (DMC)	Guardiola and Navarro <sup>16</sup>	-0.00885(1)	TTY (VMC)	this work
-0.009577	TTY	Sandhas et al. <sup>13</sup>	-0.00995(2)	TTY (DMC)	this work
-0.009619	LM2M2	Sandhas et al. <sup>13</sup>	-0.01119(4)	SAPT <sup>b</sup> (DMC)	this work
-0.00917	TTY	Salci et al. <sup>18</sup>	-0.01198(4)	SAPT (DMC)	this work
-0.01128	SAPT <sup>b,c</sup>	Suno et al. <sup>19</sup>			
-0.01132	SAPT <sup>b</sup>	Suno et al. <sup>19</sup>			

<sup>a</sup>For Monte Carlo calculations, labeled as VMC or DMC, the uncertainty on the last digit is in parentheses. <sup>b</sup>Retardation effects included into the bare SAPT potential. <sup>c</sup>Three-body effects included into the bare SAPT potential.

studies however were not conclusive due to the poor quality of the helium–helium interaction potentials available at that time.

Esry et al.<sup>10</sup> investigated the  $J = 0$  spectrum of the helium trimers using the adiabatic hyperspherical method employing the LM2M2 with add-on potential developed by Aziz and Slaman.<sup>22</sup> They established that  $^3\text{He}^4\text{He}_2$  supports no  $J = 0$  excited states but did not investigate the geometrical properties of the bound state. This study was extended by Lee et al.<sup>23</sup> to investigate the possible existence of bound states with  $J > 0$  using the hyperspherical coordinates method in the adiabatic approximation. For  $^3\text{He}^4\text{He}_2$  the lowest  $J = 1^-$  adiabatic hyperspherical potential curve has a small well, but the direct solution of the hyper-radial equation for this curve showed that this well is too shallow to support a bound state.

Nielsen et al.<sup>11</sup> studied the structure of the helium trimers using the Faddeev approach in hyperspherical coordinates employing the LM2M2 potential. Their energies agree with other works with the same potential. On the basis of the contour diagrams of the particle density distributions in the intrinsic coordinate system they tentatively concluded that while the symmetric trimer could be assimilated to an equilateral triangle, the asymmetric trimer has an elongated triangular shape with the  $^3\text{He}$ – $^4\text{He}$  distance larger than the  $^4\text{He}$ – $^4\text{He}$  one.

Bressanini et al.<sup>12</sup> using the TTY potential<sup>24</sup> performed a study of small  $^4\text{He}$  clusters containing a  $^3\text{He}$  impurity. The first member of the series is the asymmetric cluster  $^3\text{He}^4\text{He}_2$ . They computed the distribution of the lighter isotope with respect to the geometric center of mass of the various clusters and noticed the general tendency of  $^3\text{He}$  to stay on the surface of the cluster. They found linear configurations to be important in the description of  $^3\text{He}^4\text{He}_2$  but they did not estimate geometrical properties.

Guardiola and Navarro<sup>15,16</sup> in their project to establish the stability chart of mixed  $^3\text{He}/^4\text{He}$  clusters performed variational Monte Carlo (VMC) and diffusion Monte Carlo (DMC) simulations of the asymmetric trimer using various potentials. Their energies agree with those already published, but their study was not aimed at investigating the structure.

Sandhas and co-workers<sup>13</sup> computed binding energies and scattering observables of  $^3\text{He}^4\text{He}_2$  and compared them with previous results for the symmetric  $^4\text{He}_3$  system, employing both the TTY and LM2M2 potential, that are known to give quite similar results. The geometrical properties however have not been studied.

Gou and Wang<sup>17</sup> investigated the possible existence of bound rotational excited states for the  $^3\text{He}^4\text{He}_2$  using the LM2M2 potential finding no such states. No structural properties have been reported.

Salci et al.<sup>18</sup> used a finite element method to study the symmetric and asymmetric trimers. Their energetic results for the TTY potential were in line with previous studies, but no structural properties have been computed.

Suno and Esry<sup>19</sup> using the adiabatic hyperspherical method performed an investigation of both trimers using a recently developed potential<sup>25</sup> from symmetry-adapted perturbation theory (SAPT) studying also the influence of the retardation effects and three-body terms included in the potential. Since the emphasis was on the energetics no structural data have been computed. Interestingly the ground state energies of both  $^4\text{He}_3$  and  $^3\text{He}^4\text{He}_2$  are substantially lower than other previously published calculations on these systems using the LM2M2 or the TTY potentials. It might be a genuine feature of that newly developed potential, or there might have been a problem with the computational method employed. It is also interesting to notice that, while the three-body terms included in the potential affect the computed energies by less than 0.4%, including the retardation effects raises the energies by about 7%. Suno and collaborators<sup>21</sup> recently repeated these calculations with the same potential employing a variational expansion of Gaussian functions obtaining, for the  $^3\text{He}^4\text{He}_2$  system, an energy 10% higher than the previous calculations. They attributed this discrepancy to the less accurate adiabatic hyperspherical representation.

Roudnev and Cavagnero<sup>20</sup> in their study of the sensitivity to fundamental constants of helium dimer and trimers calculations, computed the energy of these systems using a variety of potentials numerically solving the Faddeev equations, obtaining results in line with those already published. The geometrical properties have not been considered.

In summary almost all studies agree with each other regarding the energetic properties, and a few of them generally conclude that  $^3\text{He}^4\text{He}_2$  is more diffuse than the symmetric trimer. However no accurate geometrical description of the most probable geometry, along with an estimate of the average particle–particle distances and interatomic angles is available in the literature.

Table 2. Parameters and Energies of the Wave Functions Employed in This Work

parameters	${}^4\text{He}_2$	${}^4\text{He}_3$	${}^3\text{He}^4\text{He}_2$ $\varphi({}^4\text{He}-{}^4\text{He})$	${}^3\text{He}^4\text{He}_2$ $\varphi({}^3\text{He}-{}^4\text{He})$
$p_5$	1485.601	1285.788	1658.975	1783.443
$p_2$	6.146323	-2.126537	8.030349	4.901079
$p_1$	0.005390	0.4619230	0.8988034	0.6233029
$p_0$	1.013632	0.0375892	0.01446931	0.009211188
$d_0$	76.37128	93.86500	75.33337	49.86342
$d_1$	1.007803	1.0	1.0573120	1.021569
VMC energy <sup>a</sup>	-0.0009014(6)	-0.08533(1)		-0.00885(1)
DMC energy <sup>a</sup>	-0.000916(2)	-0.08793(4)		-0.00995(2)

<sup>a</sup>Energies are in  $\text{cm}^{-1}$ . In parentheses are the uncertainty on the last digits.

## METHOD

In this work the potential energy has been written as a sum of two-body interactions. Many helium–helium pair potentials have been developed in the past. In this study we employed the TTY potential, which is believed to be quite accurate and was employed by Bressanini and Morosi<sup>26</sup> in their study of the shape of the  ${}^4\text{He}_3$  system. Three body effects for the helium trimers are expected to be very small due to the small polarizability of helium and the relative large interatomic distances. This was confirmed by the calculations of Suno and Esry.<sup>19</sup> Lewerenz,<sup>27</sup> in his calculations on pure helium clusters included also a three-body term in the potential but the effect on the energies was smaller than the statistical uncertainty. From the calculations of Suno and Esry<sup>19</sup> it seems that the retardation effects, along with the choice of the potential, have a much more pronounced effect on the energy than the three body effects. Unfortunately at present a direct experimental measure of the energy and the geometrical parameters of the helium trimers are still lacking, which makes the evaluation of the relative quality of the various developed helium–helium potentials more difficult. Since quantum Monte Carlo methods can simulate the exact ground state wave function, given an interaction potential, a detailed study of the sensitivity of the energy and the various geometrical parameters computed in this work, employing different potential energy surfaces and different correction terms, will be the subject of a future work.

For the above reasons we have not included, at present, three-body terms into the employed TTY potential. Atomic masses were taken from the NIST database.<sup>28</sup>

We approximate the ground state wave functions of the helium trimers with the pair-product form

$$\Psi_{\text{T}}(\mathbf{R}) = \phi_{12}(r_{12}) \phi_{13}(r_{13}) \phi_{23}(r_{23}) \quad (1)$$

where  $r_{ij}$  is the distance between two atoms and  $\phi_{ij}(r_{ij})$  is the pair function describing their interaction. In the case of the  ${}^4\text{He}_3$  system all the pair functions must be equal for symmetry reasons, while for the  ${}^3\text{He}^4\text{He}_2$  trimer only the pair functions for the  ${}^3\text{He}-{}^4\text{He}$  interactions must be equal while the  ${}^4\text{He}-{}^4\text{He}$  pair function can be independently optimized. In a previous study on rare gases trimers<sup>26</sup> we employed the pair function

$$\phi(r) = \exp\left(-\frac{p_5}{r^5} - \frac{p_2}{r^2} - p_0 \ln(r) - p_1 r\right) \quad (2)$$

that has been used with success by several workers<sup>12,27,29</sup> for the description of small rare gas clusters. We recently showed<sup>30</sup> that this functional form however does not describe accurately the wave function of the helium dimer in the repulsive region,

and we introduced a new functional form that gives a better description of that system

$$\phi(r) = \exp\left(-d_0 e^{-d_1 r} - \frac{p_5}{r^5} - \frac{p_2}{r^2} - p_0 \ln(r) - p_1 r\right) \quad (3)$$

The variational energy of this functional form recovered 98% of the exact energy of the helium dimer, therefore we decided to employ it even for the description of the helium trimers.

The chosen form for the trial wave function makes it impossible to compute analytically the matrix element of the Hamiltonian operator, so the variational energy and other properties must be computed by a numerical method like the VMC.<sup>31,32</sup> The VMC approach poses no restrictions on the functional form of the trial wave function, requiring only the evaluation of the wave function value, its gradient, and its Laplacian, and these are easily computed. Although the VMC approach, with a proper choice of the trial wave function, can give very good results by itself, in this work it has been mainly used to optimize good trial functions to be subsequently employed in a diffusion Monte Carlo (DMC) simulation. Both methods are well described in the literature<sup>32</sup> and we do not discuss them further.

All parameters in our wave function were optimized by minimizing the energy. The optimized trial wave functions  $\Psi_{\text{T}}$  were then employed in DMC calculations performed using imaginary time steps  $\tau$  of 10, 50, 100, 200, and 400 hartree<sup>-1</sup>. The time step bias has been eliminated by a linear extrapolation to  $\tau \rightarrow 0$ . All the simulations have been performed using from 10,000 to 50,000 walkers, to minimize the population control bias.

For nodeless systems, like those studied here, DMC can estimate the exact ground state energy within the desired statistical accuracy. However, expectation values of operators  $\hat{O}$  that do not commute with the Hamiltonian are approximated, since they are computed with respect to the distribution  $\Psi_{\text{T}}(\mathbf{R})\phi_0(\mathbf{R})$ , called the *mixed distribution*, and not with respect to the square of the exact wave function  $\phi_0^2(\mathbf{R})$ . For these properties we give a better estimate, which is second order on the error of the trial wave function, using the so-called second order estimate  $\langle \hat{O} \rangle \cong 2\langle \hat{O} \rangle_{\text{DMC}} - \langle \hat{O} \rangle_{\text{VMC}}$ . There are more advanced algorithms available in the literature to estimate expectation values of a generic operator  $\hat{O}$ , but for reasons explained in the next section we found this simple estimate to be accurate enough for the purposes of estimating structural properties.

To get an insight on the structure of a  ${}^3\text{He}^4\text{He}_2$ , we computed the average values of various distances and angles. For floppy systems however an average property is not necessarily representative of the physical system if the probability distribution of that property is rather broad. For



this reason we also computed the distribution functions of the relevant geometric features. Furthermore it has been already shown<sup>26</sup> that, for floppy systems, two-dimensional distributions can be very helpful to gain a better understanding of the structure. In particular in this work we computed the distribution of two out of three angles of the triangle. Fixing two angles automatically defines the third one. This distribution was used<sup>26</sup> with success to discuss the shape of  ${}^4\text{He}$ ,  ${}^{20}\text{Ne}$ , and  ${}^{40}\text{Ar}$  trimers.

## RESULTS AND DISCUSSION

We performed VMC and DMC simulations of the ground state for  ${}^4\text{He}_2$ ,  ${}^4\text{He}_3$ , and  ${}^3\text{He}^4\text{He}_2$  using trial wave functions optimized by minimizing the variational energy. The corresponding VMC and DMC energies, in  $\text{cm}^{-1}$ , along with the variational parameters of the wave functions employed in this work, are listed in Table 2.

For  ${}^4\text{He}_2$  using a previously optimized wave function we obtained a VMC energy of  $-0.0009014(6) \text{ cm}^{-1}$ . After eliminating the time step bias in DMC we obtained an energy of  $-0.000916(2) \text{ cm}^{-1}$  in optimal agreement with the numerical calculation, using the same potential, of  $-0.0009168 \text{ cm}^{-1}$  by Geltman.<sup>33</sup>

For  ${}^4\text{He}_3$  we computed a VMC energy of  $-0.08533(1) \text{ cm}^{-1}$  recovering 97% of the total energy. This is a substantial improvement compared with the quality of the wave function used in our previous study.<sup>26</sup> To our knowledge this is the most accurate compact wave function available in the literature for the pure helium trimer for the TTY potential. After correcting for the time step bias we estimate the ground state energy to be  $-0.08793(4) \text{ cm}^{-1}$  in agreement with previous calculations with the TTY potential.

Finally, for the  ${}^3\text{He}^4\text{He}_2$  trimer, our trial wave function has a VMC energy of  $-0.00885(1) \text{ cm}^{-1}$ . To remark on the very good quality of the employed trial wave function, we notice that in our earlier study<sup>12</sup> of mixed  ${}^3\text{He}/{}^4\text{He}$  clusters the wave function employed had a VMC energy of  $-0.00666(2) \text{ cm}^{-1}$ . Using our improved trial wave function we estimated the ground state energy by DMC, after eliminating the time step bias, to be  $-0.00995(2) \text{ cm}^{-1}$ .

There is roughly 1 order of magnitude of difference in energy by going from the helium dimer to the asymmetric trimer and another order of magnitude by going to the symmetric helium trimer. It is known that  ${}^3\text{He}$  and  ${}^4\text{He}$  do not form a bound dimer due to the light mass of  ${}^3\text{He}$ . This roughly means that in  ${}^3\text{He}^4\text{He}_2$ , out of three pair interactions, only the one between the two  ${}^4\text{He}$  is supporting the binding, while the  ${}^3\text{He}$  atom interacting with two  ${}^4\text{He}$  atoms lowers the ground state energy with respect to the dimer. In the  ${}^4\text{He}_3$  system instead the binding is stronger since it is shared between all pairs of interactions.

For all the systems studied here the VMC distribution functions were very similar if not superimposable to the DMC distributions, another sign of the high quality of the trial wave functions employed. In this case the use of the second order estimator, whose distributions are shown in the figures, is justified since it corrects most of the remaining deviations from the exact distribution. In cases where the wave function is not of good enough quality, one could resort to the more elaborate and time-consuming descendent weighting algorithm to estimate the distributions with respect to  $\phi_0^2(\mathbf{R})$  or similar algorithms. A drawback of this more advanced algorithm

however is that, while the expectation values converge to the exact values, their statistical uncertainty could quickly diverge. Furthermore it is much more cumbersome to implement when estimating one and two-dimensional distributions.

In Figure 1 we show the pair distribution functions, that is, the probability that two particles are at a certain distance. For

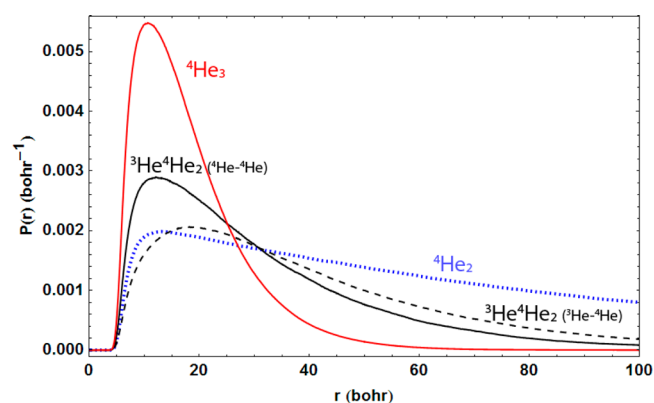


Figure 1. Pair distributions for  ${}^4\text{He}_2$ ,  ${}^4\text{He}_3$ , and  ${}^3\text{He}^4\text{He}_2$ .

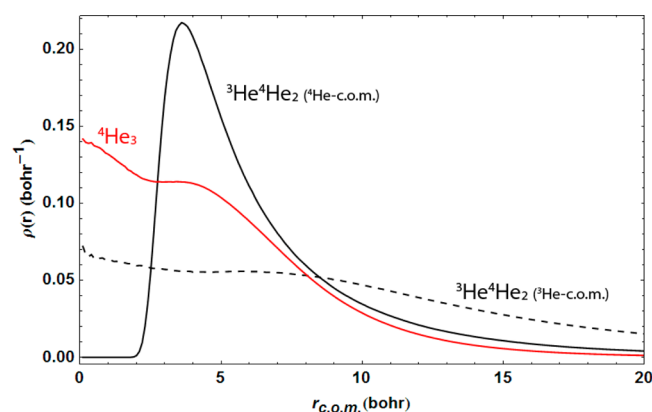
${}^3\text{He}^4\text{He}_2$  we plot both the  ${}^4\text{He}$ – ${}^4\text{He}$  pair distribution (black solid line) and the  ${}^3\text{He}$ – ${}^4\text{He}$  pair distribution (black dashed line) along with the  ${}^4\text{He}_2$  (blue dotted line) and  ${}^4\text{He}_3$  (red solid line) pair distribution functions. The  ${}^4\text{He}_3$  distribution is the least broad of the four curves with a maximum at about 10.6 bohr. However this trimer is not at all a rigid system as can be inferred from the rather large width of the curve. The broader of the curves is the one for  ${}^4\text{He}_2$ , having an extremely long tail. It is possible to find a pair of particles even as apart as 500 bohr (not shown in the plot).

We observed above that the asymmetric trimer  ${}^3\text{He}^4\text{He}_2$  has an energy between  ${}^4\text{He}_2$  and  ${}^4\text{He}_3$  so it is interesting to compare its pair distribution functions with those systems. Both the  ${}^4\text{He}$ – ${}^4\text{He}$  and the  ${}^3\text{He}$ – ${}^4\text{He}$  curves are considerably broader than the  ${}^4\text{He}_3$  one. The immediate interpretation is that the mixed trimer is an even floppier and diffuse system than  ${}^4\text{He}_3$ . The maximum of the  ${}^4\text{He}$ – ${}^4\text{He}$  curve is at 12.1 bohr with an average of 31.8 bohr, to be compared with 10.6 bohr of the symmetric system, but the tail of the curve extends at a much larger distances compared with  ${}^4\text{He}_3$ . The  ${}^3\text{He}$ – ${}^4\text{He}$  pair distribution function has a maximum at 18.2 with an average of 41.1 bohr and it is even more diffuse, even if not as diffuse as the curve of the dimer. These data and curves neatly show that looking at average values only can be misleading for floppy systems, since the average values and the most probable values can be quite different. The geometrical data are collected in Table 3.

Many previous studies of the  ${}^4\text{He}_3$  system employed the radial density with respect to the geometric center of mass (c.o.m.) in the discussion of its structural properties. This curve for systems like  $\text{Ar}_3$  and  $\text{Ne}_3$  is strongly peaked around an average value, as can be expected for an almost rigid equilateral triangle. The maximum of the  ${}^4\text{He}_3$  curve instead, (red solid line in Figure 2) is located at zero with a pronounced shoulder at about 4 bohr. The common interpretation of this peculiar plot is that nearly linear configurations, that is, where one particle is close to the geometric center of mass, contribute to the structural description of this very floppy system. In the asymmetric trimer  ${}^3\text{He}^4\text{He}_2$  we must separately analyze the density with respect the c.o.m. of  ${}^3\text{He}$  and  ${}^4\text{He}$ . The black solid

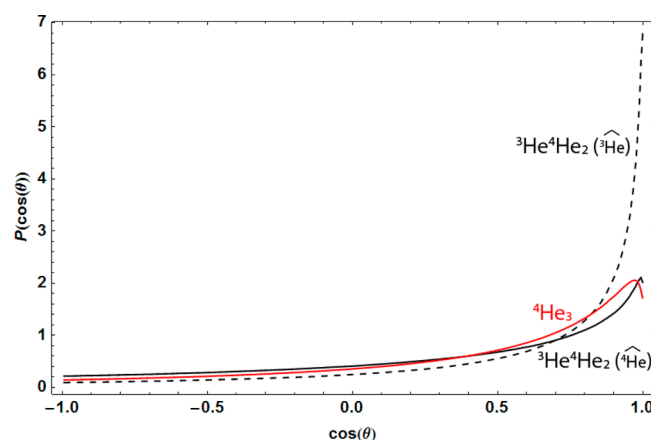
**Table 3.** Average and Most Probable Values of Various Geometrical Quantities of  ${}^4\text{He}_2$ ,  ${}^4\text{He}_3$ , and  ${}^3\text{He}^4\text{He}_2$ . Distances are Measured in bohr

system	$\langle r_{ij} \rangle$	most probable $r_{ij}$	$\langle \theta \rangle$	most probable $\theta$
${}^4\text{He}_2$	96.7	13.8		
${}^4\text{He}_3$	18.2	10.6	60°	35°
${}^3\text{He}^4\text{He}_2$	31.8 $r_{4\text{He}-4\text{He}}$	12.1 $r_{4\text{He}-4\text{He}}$	66° angle ${}^3\text{He}-{}^4\text{He}-{}^4\text{He}$	39° angle ${}^3\text{He}-{}^4\text{He}-{}^4\text{He}$
	41.1 $r_{3\text{He}-4\text{He}}$	18.2 $r_{3\text{He}-4\text{He}}$	48° angle ${}^4\text{He}-{}^3\text{He}-{}^4\text{He}$	17° angle ${}^4\text{He}-{}^3\text{He}-{}^4\text{He}$

**Figure 2.** Radial density distributions for  ${}^4\text{He}_3$  and  ${}^3\text{He}^4\text{He}_2$ .

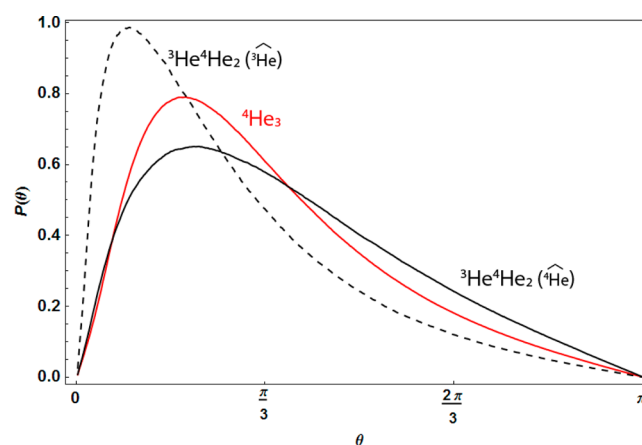
line in Figure 2 shows the curve for  ${}^4\text{He}$ : it is peaked at about 4.7 bohr and it goes to zero at 2 bohr. This means that configurations where one  ${}^4\text{He}$  is close to the c.o.m. of the system, that is, between the other  ${}^4\text{He}$  and  ${}^3\text{He}$ , are not present. On the other hand the density of  ${}^3\text{He}$  shows a slight maximum at zero and it is quite flat for at least 10 bohr, with a slowly decaying tail. An immediate interpretation of this plot is that the lighter  ${}^3\text{He}$  atom can be found at a much larger distance from the c.o.m. than the two heavier  ${}^4\text{He}$ , due to its slowly decaying tails, but also close to the c.o.m. and even just in the middle of a quasi-linear configuration. This does not mean however that these linear configurations are as probable as the configurations where the lighter  ${}^3\text{He}$  atom is far away. This plot represents a density, not a probability. The actual probability to find a configuration is divided by the corresponding phase space volume element. Even if the density is quite flat there are much more configurations where the  ${}^3\text{He}$  atom is far away. Note also that all the quasi-linear configurations where the fermionic helium is far from the other two helium atoms do not show up in this plot because we plot the density with respect to the center of mass.

We now take a look at the angles of this system. Figure 3 shows the cosine distributions for the both trimers. The cosine distribution of  ${}^4\text{He}_3$  (red solid line), already discussed,<sup>26</sup> reflects the floppy nature of this system, without a true equilibrium structure. It extends all the way from  $-1$  to  $+1$  with a maximum close, but not exactly, to  $+1$ . Since a cosine of  $+1$  corresponds to an angle of zero this curve suggests that nearly linear configurations are important in the description of the system. In the  ${}^3\text{He}^4\text{He}_2$  system there are two geometrically distinct angles. The curve for the angle centered on  ${}^4\text{He}$  (black solid line) is similar to the one of the pure trimer, only with the maximum slightly closer to  $+1$ . The cosine distribution of the angle with  ${}^3\text{He}$  at a vertex (dashed line) has a maximum right at  $+1$ , at least with the employed resolution of the statistical analysis (0.06). This means that it is more probable to find a linear configuration where one  ${}^4\text{He}$  is somewhere in the middle rather than when  ${}^3\text{He}$  is between the two heavier atoms. This is

**Figure 3.** Cosine distributions for  ${}^4\text{He}_3$  and  ${}^3\text{He}^4\text{He}_2$ .

not in contradiction with the previous graphs since the phase space available to the configurations where the  ${}^3\text{He}$  is far away is much greater than that where  ${}^3\text{He}$  is in the middle. The average cosine for the angle with  ${}^4\text{He}$  at its vertex is 0.35 while that for the angle at  ${}^3\text{He}$  is 0.58. The average cosine value for the pure  ${}^4\text{He}_3$  trimer is 0.43.

The same picture emerges examining the curves for the angular distributions shown in Figure 4, which is probably

**Figure 4.** Angular distributions for  ${}^4\text{He}_3$  and  ${}^3\text{He}^4\text{He}_2$ .

somewhat easier to interpret. The angle distribution for the symmetric trimer is peaked at about 35°, with an average of 60° due to the constraint that the sum of the three equivalent angles in a triangle is equal to 180°. For  ${}^3\text{He}^4\text{He}_2$  the curve for the angle with  ${}^4\text{He}$  at its vertex has a maximum close to 39° with 66° as an average, while the angle with the lighter helium at its vertex is 17°, with 48° as average. This is coherent with the previous observation that  ${}^3\text{He}$  can be found far away from the other two atoms. Note that again the most probable value is quite different from the average value.

A natural way to discuss the shape of any trimer is using an angle–angle two-dimensional distribution function, and this is trivially done in a Monte Carlo simulation. This distribution gives the probability to find the first angle at a given value and the second at another one, and this leads to a natural pictorial interpretation of the global shape. A two-dimensional array is set up during the simulation and the values of two angles of the instantaneous atomic configuration are collected. This procedure leads naturally to a distribution function that gives the probability to find the triangle with particular values of all the angles, the third angle being automatically fixed by the other two.

While the distribution of a more rigid trimer like  $^{40}\text{Ar}_3$  is strongly peaked around the average angle values ( $60^\circ$ ,  $60^\circ$ ) and goes quickly to zero moving away from the maximum,<sup>26</sup> the distributions of  $^4\text{He}_3$  and  $^3\text{He}^4\text{He}_2$  are quite different. The shape of the angle–angle distribution function for  $^4\text{He}_3$  shown in Figure 5 has a weakly pronounced maximum located at about

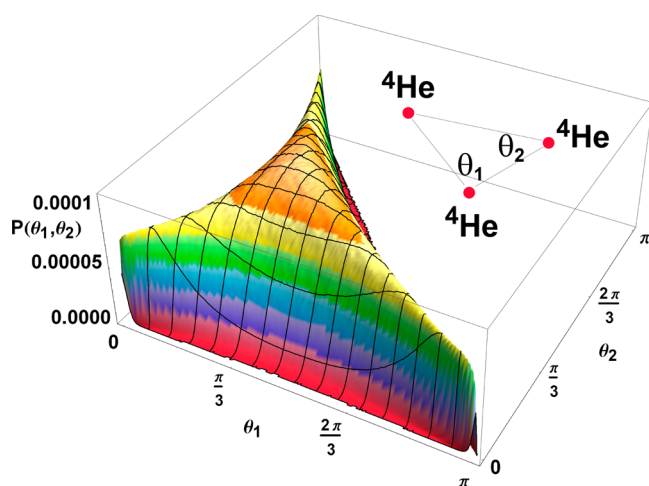


Figure 5. Angle–angle distribution function for  $^4\text{He}_3$ .

( $60^\circ$ ,  $60^\circ$ ), but the distribution is almost flat, extending in all direction with slowly decaying probabilities such that almost all possible angle pairs, including quasilinear configurations, are reached.

For the  $^3\text{He}^4\text{He}_2$  trimer the angles considered in the plot of Figure 6 are the two with a  $^4\text{He}$  at the vertex. The weak maximum present in the  $^4\text{He}_3$  plot transforms, in the  $^3\text{He}^4\text{He}_2$  plot, into a slightly curved ridge that extends from ( $0^\circ$ ,  $180^\circ$ ) to ( $180^\circ$ ,  $0^\circ$ ), that is, the configurations where the three atoms are collinear with the lighter isotope at one of the edges.

An examination of a contour plot of Figure 7 shows that the a very weakly pronounced maximum, on this ridge, is at about ( $80^\circ$ ,  $80^\circ$ ), which means that the third angle is about  $20^\circ$ . These peculiar plots of the two helium trimers describe precisely the way these systems are floppy: all kinds of configurations must be taken into account in the description of these very diffuse systems. These systems explore almost all possible configurations with probability roughly of the same order of magnitude and, while the asymmetric trimer is likely to be found with the lighter helium isotope at a larger distance from the other two, there is not a predominant preferred shape, neither equilateral nor linear nor any other particular shape.

At first it might seem puzzling that the maxima of the angle–angle distribution functions have a different value from the one shown in the angle distributions of Figures 3 and 4. However,

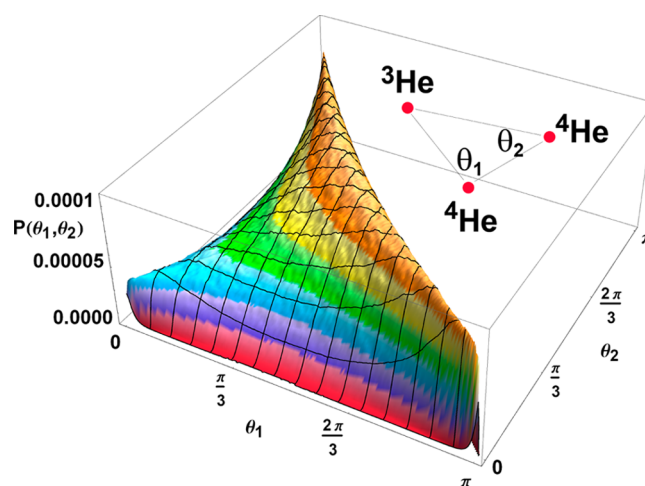


Figure 6. Angle–angle distribution function for  $^3\text{He}^4\text{He}_2$ .

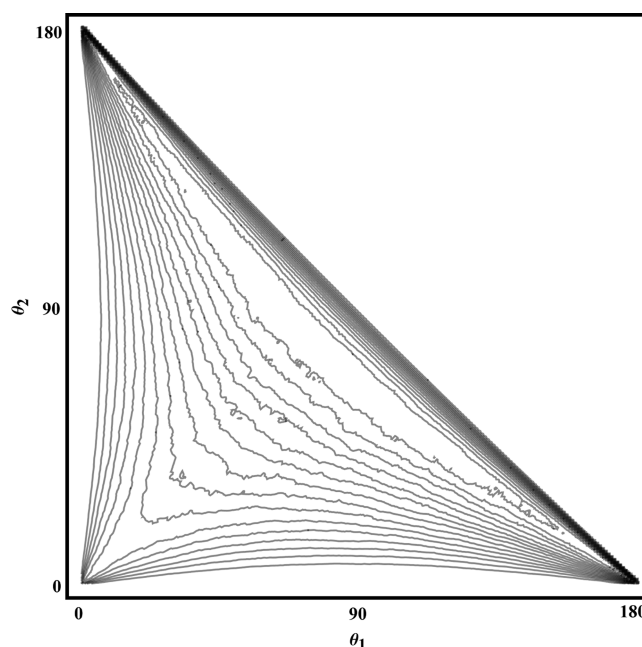


Figure 7. Contour plot of the angle–angle distribution function for  $^3\text{He}^4\text{He}_2$ . Angles in degrees.

there is no contradiction: the maximum of the angle–angle distribution function is a single point, while for each angular value of the one-dimensional distribution many configurations with lower probability can contribute to the integral. Once again this is an effect due to the phase space volume.

The TTY potential employed in this study has been widely used in these two decades to study helium clusters since it is considered to be quite accurate. Since accurate experimental results for small helium clusters, like the trimers, are still lacking, theoretical papers usually compare their results with other computational studies employing the same potential, as we have done here. However, since its introduction in 1995, many other helium–helium potentials have been proposed and it is not known, at the moment, the degree of sensitivity of the properties of small helium clusters to the exact shape of the potential. In a recent paper Hiyama and Kamimura<sup>34</sup> computed the binding energy and the average interparticle distance of the helium dimer using seven different helium–helium potentials,



including older potentials like the TTY and LM2M2 and more recent ones like the SAPT potential<sup>25</sup> employed by Suno and Esry<sup>19</sup> and by Suno et al.<sup>21</sup> in their study of  $^3\text{He}^4\text{He}_2$ . It is clear that the binding energy of the helium dimer is very sensitive to the choice of the potential, ranging from 1.3 mK to 1.7 mK, a 30% difference. Even the average interparticle distance is sensitive, ranging from 45.45 Å to 51.87 Å.

At the moment an analogous study for the helium trimers has not been done yet and it is beyond the scope of the present paper. To accurately estimate the various geometrical properties using different potentials, all trial wave functions should be separately optimized for each potential, and this is a time-consuming process. However given the contrasting results available in the literature for the SAPT potential<sup>25</sup> when applied to the  $^3\text{He}^4\text{He}_2$  system, we decided to perform additional DMC simulations, using this potential, with and without the retardation effects, without reoptimizing the trial wave functions. Since the extrapolated DMC energy is not sensitive to the choice of the employed trial wave function we are able to directly compare our results with those of Suno and Esry<sup>19</sup> and of Suno et al.<sup>21</sup>

For the ground state of  $^3\text{He}^4\text{He}_2$  using the SAPT potential,<sup>25</sup> including or excluding the retardation effects, we estimate the energy respectively to be  $-0.01119(4) \text{ cm}^{-1}$  and  $-0.01198(4) \text{ cm}^{-1}$ . We confirm that both potentials are more binding than the TTY potential, similarly to the helium dimer case.<sup>34</sup> Our results agree very well with the results of Suno and Esry<sup>19</sup> computed using the adiabatic hyperspherical representation, and not with the preliminary results of Suno et al.<sup>21</sup> using the Gaussian expansion method. We also computed the second order estimation of the pair distribution functions and the angular distributions. Since the trial wave functions have not been optimized for these potentials, these estimates of the geometrical structure can only be used, at the moment, to show a qualitative difference with those obtained here with the TTY potential. The average interparticle distances are smaller by about 10% for the bare SAPT potential and by about 8% for the SAPT potential with retardation effects included with respect to those computed using the TTY potential. On the other hand the distribution functions of the angles have not changed with respect to the TTY potential. It seems that the effect of these more attractive potentials is to shrink the distances by a few percent but the overall shape remains unchanged. We did not pursue the comparison further since a comparison between different potentials is beyond the scope of this work.

The recently published potential by Cencek et al.<sup>35</sup> is claimed to be the most accurate helium–helium potential published to date. Work is in progress in our laboratory to compute the structural parameters of the two helium trimers using this new potential and compare them with other potentials in order to explore the sensitivity of the geometrical properties to the shape of the potential curve.

## CONCLUSIONS

We optimized, using VMC, trial wave functions for  $^4\text{He}_2$ ,  $^4\text{He}_3$ , and  $^3\text{He}^4\text{He}_2$ . The resulting, high quality wave functions have been subsequently employed in DMC simulations, using the TTY potential, estimating the exact ground state energies. We computed many average geometrical properties and geometric probability distributions for the  $^3\text{He}^4\text{He}_2$  system and compared them with those of  $^4\text{He}_2$  and  $^4\text{He}_3$ . The  $^3\text{He}$  isotope, being lighter than the other two atoms, has a more diffuse probability distribution with respect to the center of mass of the system, a

fact confirmed also considering the angular distribution functions. We computed the angle–angle two-dimensional distribution to better interpret the geometrical shape of this trimer. Its analysis shows a very weakly pronounced maximum at about  $(80^\circ, 80^\circ)$ , with the third angle being about  $20^\circ$ . However the distribution extends in all directions covering roughly all possible shapes before going to zero almost at the boundaries. This means that the  $^3\text{He}^4\text{He}_2$  system cannot be classified as having any particular shape, since in this case the intuitive notion of equilibrium structure is ill defined. We hope that our analysis of the fragile asymmetric helium trimer can help experimentalists to investigate its properties in future experiments.

## AUTHOR INFORMATION

### Corresponding Author

\*E-mail: dario.bressanini@uninsubria.it.

### Notes

The authors declare no competing financial interest.

## REFERENCES

- (1) Toennies, J. P. Helium clusters and droplets: Microscopic superfluidity and other quantum effects. *Mol. Phys.* **2013**, *111* (12–13), 1879–1891.
- (2) Kolganova, E. A.; Motovilov, A. K.; Sandhas, W. The  $^4\text{He}$  trimer as an Efimov system. *Few-Body Syst.* **2011**, *51* (2–4), 249–257.
- (3) Luo, F.; McBane, G. C.; Kim, G.; Giese, C. F.; Gentry, W. R. The weakest bond: Experimental observation of helium dimer. *J. Chem. Phys.* **1993**, *98* (4), 3564–3567.
- (4) Schöllkopf, W.; Toennies, J. P. Nondestructive mass selection of small van-der-Waals clusters. *Science* **1994**, *266* (5189), 1345–1348.
- (5) Schöllkopf, W.; Toennies, J. P. The nondestructive detection of the helium dimer and trimer. *J. Chem. Phys.* **1996**, *104* (3), 1155–8.
- (6) Bruch, L. W.; McGee, I. J. Calculations and estimates of the ground state energy of helium trimers. *J. Chem. Phys.* **1973**, *59* (1), 409–13.
- (7) Brühl, R.; Kalinin, A.; Kornilov, O.; Toennies, J. P.; Hegerfeldt, G. C.; Stoll, M. Matter wave diffraction from an inclined transmission grating: Searching for the elusive  $^4\text{He}$  trimer Efimov state. *Phys. Rev. Lett.* **2005**, *95* (6), 063002.
- (8) Duffy, K.; Lim, T. K. Mixed and fermionic helium trimers. *J. Chem. Phys.* **1979**, *70* (10), 4778–81.
- (9) Nakaichi, S.; Lim, T. K.; Akaishi, Y.; Tanaka, H. Few-atom  $^3\text{He}$ – $^4\text{He}$  mixed molecules. *J. Chem. Phys.* **1979**, *71* (11), 4430–3.
- (10) Esry, B. D.; Lin, C. D.; Greene, C. H. Adiabatic hyperspherical study of the helium trimer. *Phys. Rev. A* **1996**, *54* (1), 394–401.
- (11) Nielsen, E.; Fedorov, D. V.; Jensen, A. S. The structure of the atomic helium trimers: Halos and Efimov states. *J. Phys. B* **1998**, *31* (18), 4085–105.
- (12) Bressanini, D.; Zavaglia, M.; Mella, M.; Morosi, G. Quantum Monte Carlo investigation of small  $^4\text{He}$  clusters with a  $^3\text{He}$  impurity. *J. Chem. Phys.* **2000**, *112* (2), 717–722.
- (13) Sandhas, W.; Kolganova, E. A.; Ho, Y. K.; Motovilov, A. K. Binding energies and scattering observables in the  $^4\text{He}_3$  and  $^3\text{He}^4\text{He}_2$  three-atomic systems. *Few-Body Syst.* **2004**, *34* (1), 137–142.
- (14) Kalinin, A.; Kornilov, O.; Schöllkopf, W.; Toennies, J. P. Observation of mixed Fermionic-bosonic helium clusters by transmission grating diffraction. *Phys. Rev. Lett.* **2005**, *95* (11), 113402.
- (15) Guardiola, R.; Navarro, J. Stability of small mixed clusters of  $^4\text{He}$  and  $^3\text{He}$  atoms. *Phys. Rev. Lett.* **2002**, *89* (19), 193401.
- (16) Guardiola, R.; Navarro, J. Stability chart of small mixed  $^4\text{He}$ – $^3\text{He}$  clusters. *Phys. Rev. A* **2003**, *68* (5), 055201.
- (17) Gou, B. C.; Wang, F. Weakly bound triatomic  $^4\text{He}_2^3\text{He}$  and  $^3\text{He}_2^4\text{He}$  molecules. *Int. J. Quantum Chem.* **2005**, *101* (2), 169–173.

- (18) Salci, M.; Yarevsky, E.; Levin, S. B.; Elander, N. Finite element investigation of the ground states of the helium trimers  $^4\text{He}_3$  and  $^4\text{He}_2\text{-}^3\text{He}$ . *Int. J. Quantum Chem.* **2007**, *107* (2), 464–468.
- (19) Suno, H.; Esry, B. D. Adiabatic hyperspherical study of triatomic helium systems. *Phys. Rev. A* **2008**, *78* (6), 062701.
- (20) Roudnev, V.; Cavagnero, M. Benchmark helium dimer and trimer calculations with a public few-body code. *J. Phys. B* **2012**, *45* (2), 025101.
- (21) Suno, H.; Hiyama, E.; Kamimura, M. Theoretical study of triatomic systems involving helium atoms. *Few-Body Syst.* **2013**, *54* (7–10), 1557–1560.
- (22) Aziz, R. A.; Slaman, M. J. An examination of ab initio results for the helium potential energy curve. *J. Chem. Phys.* **1991**, *94* (12), 8047–8053.
- (23) Lee, T. G.; Esry, B. D.; Gou, B. C.; Lin, C. D. The helium trimer has no bound rotational excited states. *J. Phys. B* **2001**, *34* (7), L203–L210.
- (24) Tang, K. T.; Toennies, J. P.; Yiu, C. L. Accurate analytical He–He van der Waals potential based on perturbation theory. *Phys. Rev. Lett.* **1995**, *74* (9), 1546–9.
- (25) Jeziorska, M.; Cencek, W.; Patkowski, K.; Jeziorski, B.; Szalewicz, K. Pair potential for helium from symmetry-adapted perturbation theory calculations and from supermolecular data. *J. Chem. Phys.* **2007**, *127* (12), 124303.
- (26) Bressanini, D.; Morosi, G. What is the shape of the helium trimer? A comparison with the neon and argon trimers. *J. Phys. A* **2011**, *115* (40), 10880–10887.
- (27) Lewerenz, M. Structure and energetics of small helium clusters: Quantum simulations using a recent perturbational pair potential. *J. Chem. Phys.* **1997**, *106* (11), 4596–4603.
- (28) Linstrom, P. J.; Mallard, W. G. *NIST Chemistry WebBook, NIST Standard Reference Database Number 69*; National Institute of Standards and Technology: Gaithersburg MD, 2011.
- (29) Rick, S. W.; Lynch, D. L.; Doll, J. D. A variational Monte-Carlo study of argon, neon, and helium clusters. *J. Chem. Phys.* **1991**, *95* (5), 3506–3520.
- (30) Bressanini, D. An accurate and compact wave function for the  $^4\text{He}$  dimer. *EPL* **2011**, *96* (2), 23001.
- (31) Bressanini, D.; Reynolds, P. J., Between classical and quantum Monte Carlo methods: "Variational" QMC. In *Monte Carlo Methods in Chemical Physics*, Ferguson, D. M.; Siepmann, J. I.; Truhlar, D. G., Eds. Wiley: New York, 1999; Vol. 105, pp 37-64.
- (32) Hammond, B. L.; Lester, W. A., Jr.; Reynolds, P. J., *Monte Carlo Methods in Ab Initio Quantum Chemistry*. 1st ed.; World Scientific: Singapore, 1994.
- (33) Geltman, S. Ritz variational treatment of the  $^4\text{He}$  trimer. *Eur. Phys. Lett.* **2009**, *85* (3), 33001.
- (34) Hiyama, E.; Kamimura, M., Linear correlations between  $^4\text{He}$  trimer and tetramer energies calculated with various realistic He-4 potentials. *Phys. Rev. A* **2012**, *85* (6).
- (35) Cencek, W.; Przybytek, M.; Komasa, J.; Mehl, J. B.; Jeziorski, B.; Szalewicz, K. Effects of adiabatic, relativistic, and quantum electro-dynamics interactions on the pair potential and thermophysical properties of helium. *J. Chem. Phys.* **2012**, *136* (22), 224303.